Open Access Library Journal
2022, Volume 9, e9569
ISSN Online: 2333-9721
ISSN Print: 2333-9705

Thermodynamic Analysis of Al Alloy Reinforced with Zirconia Particles

Ahmed Abdelkareem

Reactor Materials Department, Nuclear Materials Authority, Cairo, Egypt
Email: kareemnma@yahoo.com

How to cite this paper: Abdelkareem, A. (2022) Thermodynamic Analysis of Al Alloy Reinforced with Zirconia Particles. *Open Access Library Journal*, **9**: e9569.
https://doi.org/10.4236/oalib.1109569

Received: November 14, 2022
Accepted: December 27, 2022
Published: December 30, 2022

Abstract

In this paper, HSC software was used to perform a thermodynamic analysis of A5083/ZrO_2 metal matrix composite to predict the phases which formed during the manufacturing processes (vortex method). The base matrix was purchased commercially and the zirconia particles were extracted from Egyptian zircon as a reinforcing material by alkaline fusion technique. The base material was melted in an electric furnace at 750˚C, and the extracted zirconia particles were added while stirring. Thermodynamic diagrams predicted that ZrO_2 would react with the matrix to produce new phases such as MgO and Al_2O_3 in preference to the formation of MgO. Characterization of the fabricated zirconia and composites was performed by various methods; Scanning Electron Microscopy (SEM), Energy Distributed X-ray (EDS) and X-ray Diffraction (XRD). The results demonstrate successful extraction of high purity zirconia (98.85%) and fabrication of composites during stir casting. Furthermore, SEM mapping of the fabricated composite revealed the presence of MgO and Al_2O_3 consistent with thermodynamic studies.

Subject Areas

Material Science, Composite Materials

Keywords

A5083, Zirconia, Thermodynamics, Vortex Casting, Composites

1. Introduction

For the last few decades, the development of materials shifted from monolithic alloy to composite materials in order to meet the global industrial needs. Conventional alloys have limits to realize a good combination of strength, stiffness, toughness and density. To overcome these shortcomings and to meet the ever-increasing demand of modern technology, composites are the most promising materials of recent interest [1] [2] [3]. The continuous developments in composite fabrications are directed to the use of composite materials in more and more diversified applications [4] [5]. Metal matrix composites (MMCs) reinforced with ceramic materials have improvements in their mechanical properties so has a high strength and modulus, as well as good high-temperature properties, when compared with corresponding base matrix alloys. MMCs are considered promising materials for automotive and aerospace applications due to their high strength to weight ratio [6] [7].

Aluminum and its alloys are the most selected matrix for MMCs. Al alloys are quite attractive and becoming potential engineering materials having excellent combination of properties such as high specific strength, high specific stiffness, electrical and thermal conductivities, low coefficient of thermal expansion and wear resistance [7] [8] [9] [10]. Aluminum-Magnesium alloys are non-heat treatable, and they drive their strength from solid solution strengthening, grain refinement, and strain hardening. Al-Mg alloys with low Mg content have better formability and are more suitable for large wrought products [11]. Al-Mg alloys reinforced with ceramic particulates have significant potential for structural applications due to their high stiffness and specific strength as well as low density. where Mg has a density (1.7 g/cm^3) lower than density of Al (2.67 g/cm^3), alloy of Mg-Al, used recently to produce lightweight and economical products. Also, Al-Mg alloys have been reported as a promising alloy system for investigation due to their low electrode potential, and high current capacity to be used as galvanic anode.

The addition of the reinforcement enhances the mechanical properties of Al based composite, when compared to the matrix alloy. Various forms of reinforcements are used in Al matrices such as silicon carbide, alumina, and zirconia. In the form of fibers, whiskers or particulate to enhance the overall performance of alloys [12] [13]. The process for manufacturing of MMCs generally depends on the types of reinforcement. There are different methods to fabricate MMCs; liquid-state, solid-state, semi-solid state, and in situ fabrication technique. Stir casting technique is one of the promising routes for producing large size components and high-volume production with low cost [14] [15]. On the other hand, the literature [1] [2] [4]-[9] [11]-[16] showed that the fabrication of MMCs are facing some difficulties which hider the development. The non-wetting behavior between the host matrix and particles is the most critical issue in MMCs fabrication. Attempts to overcome this have usually involved the use of chemical activations or heat treatments for the reinforcement to improve the wettability and assist the infiltration.

The use and application of MMC in many technical structures is constantly increasing, and its properties can be handcrafted by modifying their constituents, matrix and reinforcement, and fabrication method. Therefore, this current work aims to predict potential reactions that may occur during the fabrication of zirconia-reinforced A5083.

2. Thermodynamic Studies

Thermodynamic data are used to predict the types of reactions that may occur between reinforcing materials and base matrix elements during casting and solidification processes. For this purpose, the chemistry software program HSC-6 is used. HSC-6 is basically used to determine the probability of formation within a matrix, whether it is an element, an oxide, or a compound, based on the chemical analysis of the matrix. Predict the probability of ZrO_2 reduction reaction to Zr metal and the stability of elements and oxides at different temperatures,

Where the base matrix for this investigated is A5083, it consists of Al and Mg as the major alloying element (5%). while, the selected reinforcement material is the prepared ZrO_2 particle. Thermodynamic stability plots of A5083 systems with different ZrO_2 percentages (5%, 10%, 15%, and 20%) are generated by HSC software as shown in Figure 1. These diagrams show the potential elements and compounds might be formed during casting and solidification.

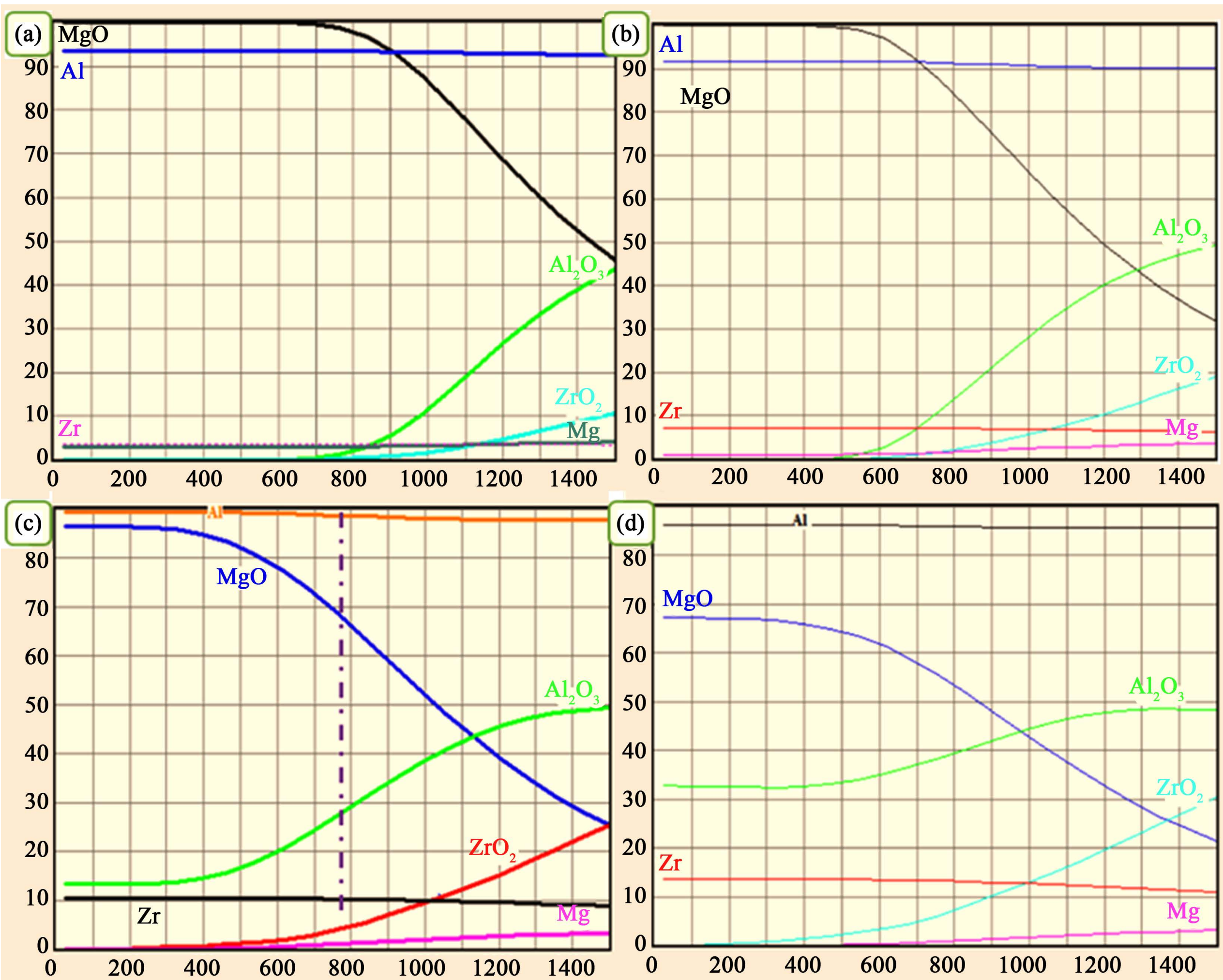

Figure 1. Thermodynamic stability diagrams. (a) composite 5% ZrO_2; (b) composite 10% ZrO_2; (c) composite 15% ZrO_2; (d) composite 20% ZrO_2. Al-Aluminium, Mg-Magnesium, Zr-Zirconium, Al_2O_3-Aluminium Oxide, MgO-Magnesium Oxide, ZrO_2-Zirconium oxide (Zirconia).

This clearly indicates the potential formation of MgO and Al_2O_3 during fabrication and solidification temperatures. Furthermore, it was revealed that the formation potential of MgO is higher than that of Al_2O_3 in the temperature range from room temperature to casting temperature (650˚C - 800˚C) as shown in **Figures 1(a)-(d)**. This behavior implies that Mg completely reacted with ZrO_2 to form MgO and Zr metal. When the ZrO_2 fraction is increased, Mg is not sufficient to react with this high ZrO_2 fraction. After Mg was consumed, Al reacted with ZrO_2 and he started to form Al_2O_3 and Zr metal. **Figure 1(c)** was chosen to illustrate the stability diagram for metals and oxides. The figure represents metals and oxides where the sum of metals (Al, Mg, Zr) equals 100% and the sum of oxides (Al_2O_3, MgO, ZrO_2) equals 100% at each temperature. Therefore, the proportions of Al, Mg, and Zr metals at the casting temperature (750˚C) are thermodynamically assumed to be about 89.2% and 9%, respectively. Similarly, the percentages of Al_2O_3, MgO, and ZrO_2 oxides are about 28.67% and 5%, respectively, at that temperature. This result indicates that about two-thirds of the added ZrO_2 is reduced to Zr metal and its oxygen combines with Al and/or Mg to form Al_2O_3 and/or MgO depending on composition and temperature. It is obviously showed the formation of MgO and Al_2O_3 during fabrication and solidification temperatures will be occur.

To determine the dominant reaction of ZrO_2 with Al or Mg, thermodynamic calculations such as enthalpy (ΔH), entropy (ΔS), and free energies (ΔG) are performed. Thermodynamic data for reaction (1) and (2) are recorded in **Table 1** and **Table 2** respectively. Its noted that the ΔG values are negative at zero temperature for both reaction which means can take place spontaneously and by increasing the temperature, the ΔG values decreased. At casting temperature

Table 1. Thermodynamic data for equation (1).

$$1.5ZrO_2 + 2Al = 1.5Zr + Al_2O_3 \quad (1)$$

Temperature ˚C	Delta (H) kJ	Delta (S) J/K	Delta (G) kJ
0	−24.841	−21.011	−19.102
100	−26.382	−25.837	−16.741
200	−27.433	−28.360	−14.014
300	−27.944	−29.355	−11.119
400	−28.190	−29.751	−8.162
500	−28.553	−30.250	−5.166
600	−29.185	−31.018	−2.102
700	−51.254	−54.677	1.955
800	−51.568	−54.985	7.439
900	−45.907	−50.016	12.770
1000	−46.948	−50.868	17.815

Table 2. Thermodynamic data for equation (2).

$ZrO_2 + 2Mg = Zr + 2MgO$ (2)			
Temperature ˚C	Delta (H) kJ	Delta (S) J/K	Delta (G) kJ
0	−102.761	−21.890	−96.781
100	−103.216	−23.330	−94.510
200	−103.509	−24.030	−92.139
300	−103.755	−24.502	−89.712
400	−104.030	−24.943	−87.239
500	−104.395	−25.446	−84.721
600	−104.905	−26.065	−82.146
700	−122.718	−45.359	−78.577
800	−123.712	−46.332	−73.991
900	−120.727	−43.722	−69.435
1000	−122.208	−44.934	−65.001

(above 700˚C), its clearly noted that ΔG value is become positive for the formation of Al_2O_3 and still negative for the formation of MgO. This means that, at casting temperature, MgO has formation priority and stability.

Moreover, clearly indicated that the formation potentials for MgO is higher than Al_2O_3 for all investigated percentages of ZrO_2 in temperature range from room temperature up to casting temperatures (650˚C - 800˚C). This behavior means that Mg fully reacted with ZrO_2 to form MgO and Zr metal. By increasing the percentage of ZrO_2, Mg become not enough to react with that higher percentage of ZrO_2. After consumable of Mg, Al began to react with ZrO_2 to form Al_2O_3 and Zr metal.

3. Experimental Work

3.1. Materials

3.1.1. Al-Alloy

The selected Al-alloy for the present investigation is the commercial alloy (A5083) with the chemical composition as shown in Table 3, maintaining the Integrity of the Specifications.

3.1.2. Reinforcement Material

The selected reinforcement material for using in production of A5083 MMCs are ZrO_2 particles. ZrO_2 particles will be prepared from the Egyptian zircon via alkaline fusion technique. Zircon is the most abundant zirconium ore and the main source for commercial production of zirconium, its compounds and alloys. The chemical composition of zircon concentrate ($ZrSiO_4$), separated from the Egyptian black sand heavy mineral from Egyptian Nuclear Materials Authority (ENMA) is shown in Table 4.

Table 3. The chemical composition of A5083 base matrix.

Element	Mn	Mg	Fe	Si	Cu	Al
%	0.46	4.22	0.23	0.35	0.09	Balance

Table 4. Average chemical composition of the concentrated Egyptian zircon.

Compound	ZrO_2	SiO_2	HFO_2	Al_2O_3	Fe_2O_3	TiO_2	Other
%	63.07	31.23	2.27	0.87	0.77	0.82	Balance

The production and applications of zirconia have continued to attract the interest of scientists and technologists. The dry and wet chemical methods are the main conventional ways for synthesizing ZrO_2 powder. The wet chemical methods (extraction with caustic alkalis, fluorides and lime) can produce high-grade zirconia because the impurities can be separated by controlled precipitation from the solutions. Various methods of decomposition have been investigated owing to the different levels of purity required and the cost of manufacture [17] [18] [19]. All these methods have three steps in common. Firstly, zircon is decomposed or dissociated by chemical, thermal or mechanochemical means. Secondly, the products obtained are treated by solubility differentiation. Thirdly, zirconium compounds are isolated from the residual impurities. Alkali fusion of zircon concentrates presents good versatility, is simple and economic process where requires low capital and operation costs [20]. These features make alkali fusion the selected method for producing zirconia particles.

Alkali fusion technique for zircon is known as zircon opening which include the following procedure which schematically represented in **Figure 2**. Firstly, mixture zircon with NaOH by ratio 1:1.35 in stainless steel crucible then fused in a Muffle furnace at 650˚C ± 10˚C for 2.5 h. The opening product (frit) consists of two major compounds Na_2SiO_3 (water soluble) and Na_2ZrO_3 in addition to some impurities and unreacted zircon. Frit was water leached to remove the impurities (sodium silicate). Hydrated sodium zirconate is obtained by filtration then followed by drying at 110˚C for 12 h. The dried frit is leached in 6 M HCl at 90˚C and left overnight to produce a jelly like mixture of silica gel and zirconium oxychloride. The products of leaching are separated by water dissolution and filtration to produce pure zirconium oxychloride solution. Pure oxychloride crystals are obtained by evaporation of the zirconium oxychloride solution then washed by acetone to remove excess chlorine. To precipitate zirconium hydroxide ($Zr(OH)_4$), the white crystals were leached with distilled water and pH was adjusted at 10 by the addition of ammonia. Next, the precipitate washed with water for several times and dried at 110˚C for 12 h followed by calcination for 1.5 h at 900˚C.

3.2. Preparation of Composite

The fabrication of MMCs was carried out by stir casting process. The base alloy

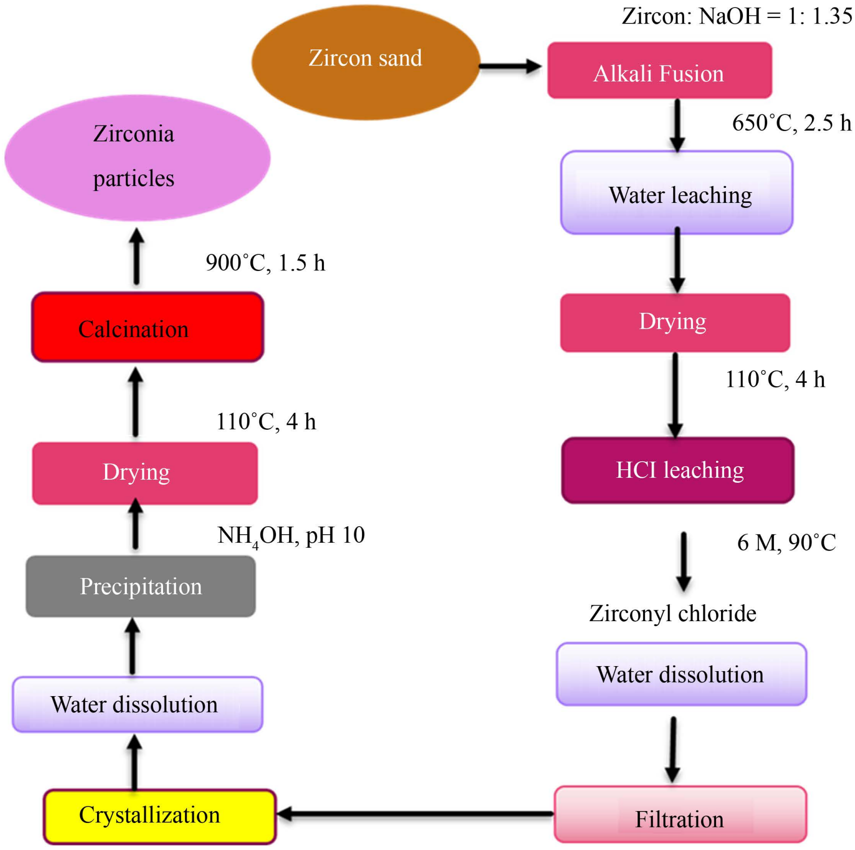

Figure 2. Synthesis procedure for zirconia preparation.

A5083 was placed in a graphite crucible inside an electrical resistance furnace. During heating, the Al alloy was melted and adjusted the casting temperature at 750˚C. After melting, the molten metal was purfacition by addition of flux. Next, the formed slag on the surface was removed carefully. This step also helped to effectively remove gases from the metal phase. The mechanical stirrer was inserted in the molten metal rotated at an impeller speed of 1200 rpm. The preheated ZrO_2 particles were gradually added to the vortex. ZrO_2 particles were heated to remove the gas layer from surface which enhances the fabriction of composoite. The presence of gas layer on the surface of particles ellimite the reaction between molten Al and ZrO_2 which in turn decreasing the wetabbility [1] [5]. The melt was continuously stirred for seven min after the addition of ZrO_2 to ensure the homogeneous distribution of the particles. Finally, the molten was poured into the permanent mold and allowed to cold in the air.

3.3. Microstructure

Scanning electron microscope (SEM) with energy dispersive X-ray spectroscopy (PHILIPS, XL 30 ESEM at 30 kV voltage) was used to characterize the microstructure of the materials. The samples were first ground on a series of SiC emery papers underwater stream, followed by polishing a series of polishing cloths with alumina suspension.

Also, X-ray diffraction analysis was performed using Philips Machine to determine the different phases of AA5083 and its composites. The XRD machine was operated at the following conditions; monochromatic Cu-K radiation with l = 0.154 nm, scanning range was 10 - 80 (2θ), and scanning step size of 0.01˚ (2θ)/Sec.

4. Results and Discussion

4.1. Preparation of ZrO_2 Particles

The preparation of Zirconia particles starts with opening-up of zircon concentrate followed by a series of hydrometallurgical and pyrometallurgical processes. Firstly, zircon is fused with sodium hydroxide at 650˚C for 2 h then cooled in the furnace. The main reactions that take place between $ZrSiO_4$ and NaOH during alkali fusion are as follows [20] [21] [22]:

$$ZrSiO_4 + 2NaOH \rightarrow Na_2ZrSiO_5 + H_2O \quad (3)$$

$$ZrSiO_4 + 4NaOH \rightarrow Na_2ZrO_3 + Na_2SiO_3 + 2H_2O \quad (4)$$

$$ZrSiO_4 + 6NaOH \rightarrow Na_2ZrO_3 + Na_4SiO_4 + 3H_2O \quad (5)$$

The product of fusion is named frit which, according to the Equations (3)-(5) consisting of sodium zirconate (Na_2ZrO_3), sodium zirconium silicate (Na_2ZrSiO_5) and sodium silicate (Na_2SiO_3, Na_4SiO_4) beside water vapor. Next, frit is washed with cold water for three times to remove both soluble silicates and excess caustic. Most of the water soluble Na_2SiO_3, Na_4SiO_4, and unreacted NaOH dissolve in water, whereas the insoluble Na_2ZrO_3 is hydrolyzed to $ZrO(OH)_2$ as per reaction (6). By filtration the solution, the filtrate consists of the soluble substances while the residue represents both $ZrO(OH)_2$ and Na_2ZrSiO_5 which are dried, then leached with HCl according to Equations (7) and (8).

$$Na_2ZrO_3 + 2H_2O \rightarrow ZrO(OH)_2 + 2NaOH \quad (6)$$

$$ZrO(OH)_2 + 2HCl \rightarrow ZrOCl_2 + 2H_2O \quad (7)$$

$$Na_2ZrSiO_5 + 4HCl \rightarrow ZrOCl_2 + 2NaCl + H_2SiO_3 + H_2O \quad (8)$$

The solution was left overnight to assist silica to precipitate in the form of silica gel, and zirconium oxychloride to crystallize. The freeze solution was dissolved in the water, then filtrate to remove silica. The filtrated solution was concentrated via volume reduction evaporation process to obtain $ZrOCl_2$ crystals as shown in **Figure 3(a)**. $ZrOCl_2$ crystals were water leached then treated with ammonium hydroxide to precipitate zirconium hydroxide as illustrated in Equation (9).

Finally, zirconium hydroxide was washed, dried and calcined at 900˚C for 1.5 h producing zirconium dioxide (ZrO_2 particles) as per Equation (10). The prepared white zirconia is shown in **Figure 3(b)**.

$$ZrOCl_2 \cdot 8H_2O + 2NH_4OH \rightarrow ZrO(OH)_2 \cdot 6H_2O + 2NH_4Cl \quad (9)$$

$$ZrO(OH)_2 \rightarrow ZrO_2 + 2H_2O \quad (10)$$

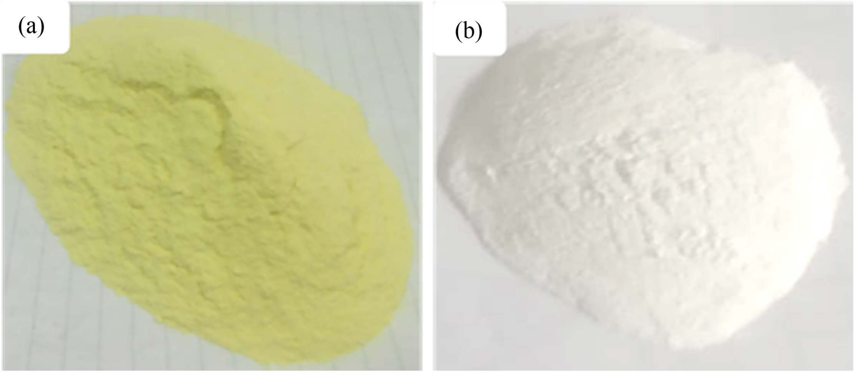

Figure 3. Zircon opening products; (a) $ZrOCl_2$ and (b) ZrO_2 powder.

SEM/EDS analysis of the prepared zirconia is shown in Figure 4. It is important to note that ZrO_2 particles have irregular shape and size as shows in Figure 4(a). However, the purity of ZrO_2 particles is about 98.85% where Si, Ca, and Cl are the accompanied impurities with 0.8%, 0.23%, 0.12% respectively as recorded in Table 5.

4.2. Microstructure

SEM images of typical microstructures of as-cast composites are shown in Figure 5. The microstructure of A5083 consisted of Al-Mg solid solution with a long arm spacing dendritic structure. The most important aspect of the microstructure is the distribution of the reinforcing particles. Achieving a uniform distribution of reinforcement is one such challenge which impacts directly on the properties and quality of the composite material. The produced MMCs containing 5 and 10 weight fractions of ZrO_2 which are wetted and well bonding to the matrix. A representative cross section of the ZrO_2 distribution in matrix is shown in Figure 5. On the other hand, the presence of the ZrO_2 decreases the arm spacing as shown in Figure 5(b) and Figure 5(c). Also, Figure 5 shows that the constituents of the base matrix and the composite are homogeneously distributed.

As shown in Figure 6, the XRD analysis shows that the base alloy consists mainly of α-Al solid solution, while the composite contains the same composition and ZrO_2 particles. It is evident that with increasing ZrO_2 particle content, the intensity of ZrO_2 peak increases and the intensity of Al peak decreases. The reducing in intensity is due to the difference in thermal expansion between the Al matrix and ZrO_2 particles. On the other hand, Al_2O_3 and/or MgO do not appear in XRD patterns. This means that the percentage is below the detection limit of XRD.

SEM mapping demonstrates the presence of Zr, O, Mg and Al as shown in Figure 7. It is clearly noted that the particle at middle of the image refers to the ZrO_2 due to that red color means Zr while green color refers to Oxygen. The presence of Oxygen surrounding the red color revealed the presence of ZrO_2. Furthermore, the presence of high concentration of green color as indicated in

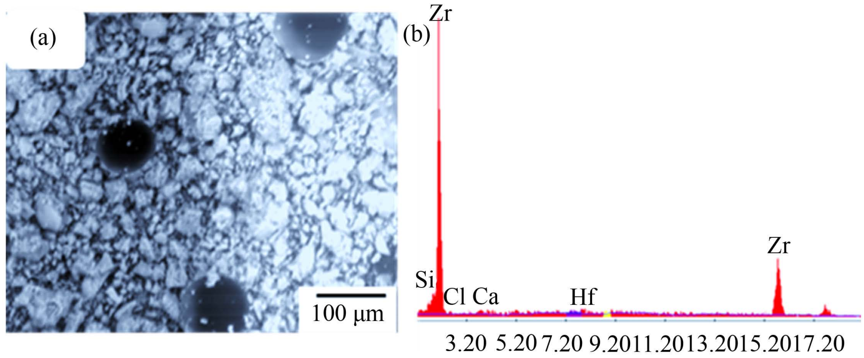

Figure 4. SEM and EDS of the prepared ZrO_2.

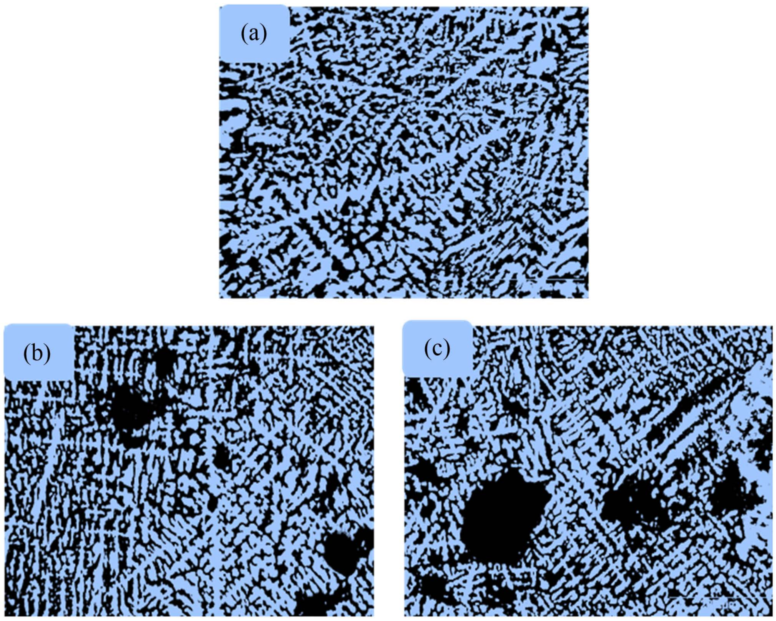

Figure 5. SEM images of (a) base alloy, (b) composite 5% ZrO_2 and (c) composite 10% ZrO_2.

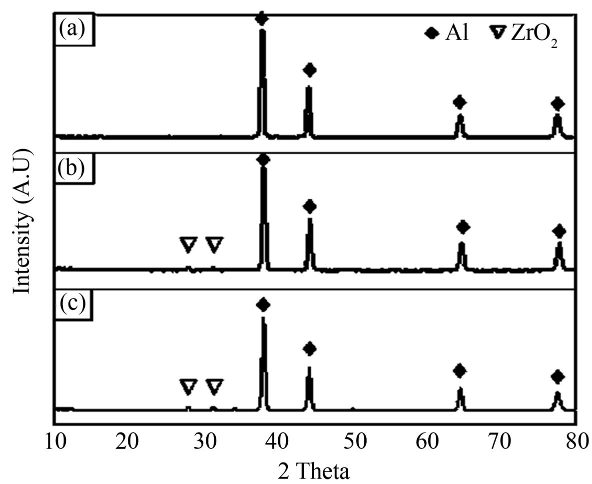

Figure 6. XRD patterns of (a) base alloy, (b) composite 5% ZrO_2 and (c) composite 10% ZrO_2.

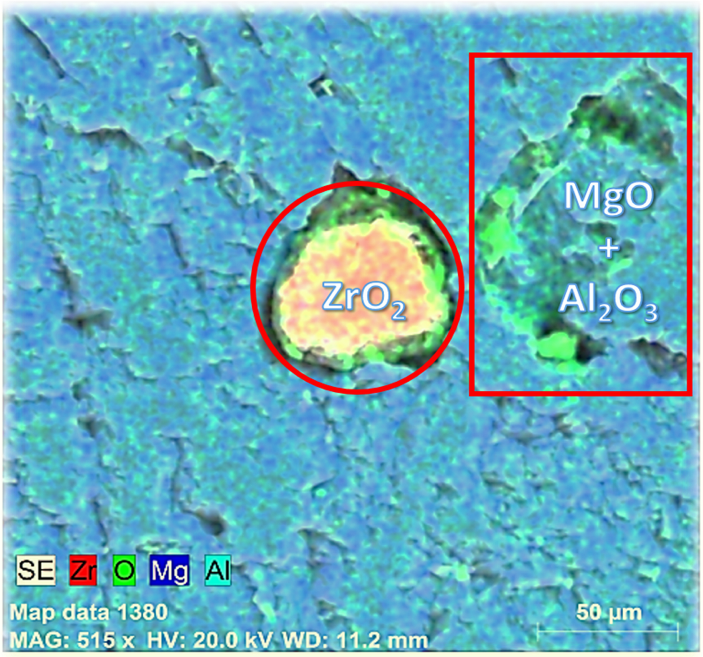

Figure 7. SEM mapping of composite 5% ZrO_2.

Table 5. EDS analysis of the prepared Zirconia.

Element	Zr	Hf	Si	Cl	Ca
%	95.88	2.97	0.8	0.12	0.23

the red rectangular means the Al and/or Mg reacted with Oxygen and formed new phases (Al_2O_3 and/or MgO).

5. Conclusions

The chemistry software HSC-6 was used to investigate the thermodynamic behavior of ZrO_2-reinforced Al alloys. The study yielded the following key findings:

1) Thermodynamic analysis results predicted that ZrO_2 would react with the base alloy to form new phases such as MgO and Al_2O_3.

2) Based on the thermodynamic stability diagram and ΔG values, the formation of MgO is the dominant reaction.

3) Succeeded in producing high-purity (98.85) zirconia by alkali fusion method.

4) Effective fabrication of Al 5083 composites reinforced with ZrO_2 particles by stir casting

5) SEM mapping approved the presence of MgO and Al_2O_3, consistent with thermodynamic studies.

Conflicts of Interest

The author declares no conflicts of interest.

References

[1] Abdizadeh, H. and Baghchesara, M.A. (2013) Investigation on Mechanical Properties and Fracture Behavior of A356 Aluminum Alloy Based ZrO_2 Particle Reinforced Metal-Matrix Composites. *Ceramics International*, **39**, 2045-2050. https://doi.org/10.1016/j.ceramint.2012.08.057

[2] Girish, K. and Shobha, B. (2018) Synthesis and Mechanical Properties of Zirconium Nano-Reinforced with Aluminium Alloy Matrix Composites. *Materials Today: Proceedings*, **5**, 3008-3013. https://doi.org/10.1016/j.matpr.2018.01.100

[3] Mohrez, W.A., Abdelkareem, A., Gamal, H. and Rashed, G.M. (2018) First Trial of SiC/SiC Tube Fabrication for Tungsten Monoblock Armor. *Journal of Radiation Research and Applied Sciences*, **11**, 242-248. https://doi.org/10.1016/j.jrras.2018.03.003

[4] Harsha, R., Kulkarni, M.V. and Babu, B.S. (2020) Study of Mechanical Properties of Aluminium/Nano-Zirconia Metal Matrix Composites. *Materials Today: Proceedings*, **26**, 3100-3106. https://doi.org/10.1016/j.matpr.2020.02.641

[5] Rashed, G., Sadawy, M., Kandil, A., Abd Elkarim, A. and Mohrez, W. (2021) Influence of ZrO_2 Particles on the Tribological Properties of AlMg5 Alloy. *Journal of Petroleum and Mining Engineering*, **23**, 95-103. https://doi.org/10.21608/jpme.2021.68312.1078

[6] Beyrami, B.P., Abdizadeh, H., Baharvandi, H. and Bonab, M. (2008) The Effect of Composition and Stir-Casting Parameters on the Mechanical Properties of Al/ZrO_2p Nanocomposites. *Proceedings of the* 13*th European Conference on Composite Materials*, Stockholm.

[7] Alaneme, K.K. and Bodunrin, M.O. (2011) Corrosion Behavior of Alumina Reinforced Aluminium (6063) Metal Matrix Composites. *Journal of Minerals and Materials Characterization and Engineering*, **10**, 1153-1165. https://doi.org/10.4236/jmmce.2011.1012088

[8] Hynes, N.R.J., Sankaranarayanan, R., Tharmaraj, R., Pruncu, C.I. and Dispinar, D. (2019) A Comparative Study of the Mechanical and Tribological Behaviours of Different Aluminium Matrix-Ceramic Composites. *Journal of the Brazilian Society of Mechanical Sciences and Engineering*, **41**, Article No. 330. https://doi.org/10.1007/s40430-019-1831-7

[9] Abbas, A., Huang, S.J., Ballokova, B. and Sülleiová, K. (2020) Tribological Effects of Carbon Nanotubes on Magnesium Alloy AZ31 and Analyzing Aging Effects on CNTs/AZ31 Composites Fabricated by Stir Casting Process. *Tribology International*, **142**, Article ID: 105982. https://doi.org/10.1016/j.triboint.2019.105982

[10] Ekuma, C., Osarolube, E., Chukwuocha, E.O. and Onyeaju, M.C. (2011) New Trends in Corrosion Analysis of Al-Sn Alloy Duplex System. *World Journal of Condensed Matter Physics*, **1**, 33-36. https://doi.org/10.4236/wjcmp.2011.12006

[11] Narain, V. and Ray, S. (2020) Comparative Study of Mechanical Properties of Cast and Forged Al-3Mg-MnO_2 and Al-8Mg-MnO_2 Composites. *Heliyon*, **6**, e03275. https://doi.org/10.1016/j.heliyon.2020.e03275

[12] Panwar, N. and Chauhan, A. (2018) Fabrication Methods of Particulate Reinforced Aluminium Metal Matrix Composite—A Review. *Materials Today: Proceedings*, **5**, 5933-5939. https://doi.org/10.1016/j.matpr.2017.12.194

[13] Marini, C.D. and Fatchurrohman, N. (2015) A Review on the Fabrication Techniques of Aluminium Matrix Nanocomposites. *Jurnal Teknologi*, **74**, 103-109. https://doi.org/10.11113/jt.v74.4840

[14] Srivastava, A.K., Gupta, Y., Patel, S., Tiwari, S.K. and Pandey, S. (2018) Metal Matrix Composites—A Review on Synthesis and Characterization. *IOP Conference Series: Materials Science and Engineering*, **691**, Article No. 012077. https://doi.org/10.1088/1757-899X/691/1/012077

[15] Suthar, J. and Patel, K. (2018) Processing Issues, Machining, and Applications of Aluminum Metal Matrix Composites. *Materials and Manufacturing Processes*, **33**, 499-527. https://doi.org/10.1080/10426914.2017.1401713

[16] Srivyas, P.D. and Charoo, M.S. (2018) A Review on Tribological Characterization of Lubricants with Nano Additives for Automotive Applications. *Tribology in Industry*, **40**, 594-623. https://doi.org/10.24874/ti.2018.40.04.08

[17] El-Kareem, A.A. (2019) New Extraction Technique of Zirconium and Hafnium from Zircon Mineral. *Arab Journal of Nuclear Sciences and Applications*, **52**, 201-208. https://doi.org/10.21608/ajnsa.2019.3052.1066

[18] De Souza, S. and Terry, B. (1994) Production of Stabilized and Non-Stabilized ZrO_2 by Carbothermic Reduction of $ZrSiO_4$. *Journal of Materials Science*, **29**, 3329-3336. https://doi.org/10.1007/BF00356681

[19] Rizzuti, A., Leonelli, C., Corradi, A., Caponetti, E., Martino, D.C., Nasillo, G. and Saladino, M. (2009) Structural Characterization of Zirconia Nanoparticles Prepared by Microwave-Hydrothermal Synthesis. *Journal of Dispersion Science and Technology*, **30**, 511-1516. https://doi.org/10.1080/01932690903123676

[20] Abdelkader, A., Daher, A. and El-Kashef, E. (2008) Novel Decomposition Method for Zircon. *Journal of Alloys and Compounds*, **460**, 577-580. https://doi.org/10.1016/j.jallcom.2007.06.032

[21] Liu, J.C., Song, J., Qi, T., Zhang, C.Q. and Qu, J.K. (2016) Controlling the Formation of Na_2ZrSiO_5 in Alkali Fusion Process for Zirconium Oxychloride Production. *Advanced Powder Technology*, **27**, 1-8. https://doi.org/10.1016/j.apt.2015.08.005

[22] Abdel-Rehim, A.M. (2005) A New Technique for Extracting Zirconium Form Egyptian Zircon Concentrate. *International Journal of Mineral Processing*, **76**, 234-243. https://doi.org/10.1016/j.minpro.2005.02.004